

THE BOUNDARY LAYER HEIGHT AND ENTRAINMENT ZONE ASSESSMENT FROM LIDAR, METEOROLOGICAL AND FORECAST MODEL DATA

Anca Nemuc¹, Camelia Talianu¹, Livio Belegante¹, Richard Ngo², Claude Derognat²

⁽¹⁾ National Institute of R&D for Optoelectronics, 409 Atomistilor Str., Magurele, Romania, anca@inoe.inoe.ro

⁽²⁾ ARIA Technologies SA, 8-10, rue de la Ferme – 92100 Boulogne Billancourt Cedex, France, mgo@aria.fr, cderognat@aria.fr,

ABSTRACT

Planetary boundary layer (PBL) processes control energy, water, and pollutant exchanges between the surface and free troposphere. Mixing height data are necessary to evaluate boundary layer transport parameterizations in numerical weather prediction models, and to relate fluxes and concentrations of gaseous and particle constituents in the atmosphere from inverse models.

In this study the top of the atmospheric mixed layer and the thickness of the entrainment zone is analyzed using lidar, meteorological (NOAA-GDAS) and numerical weather prediction model (WRF), focused on three years during 2009-2011.

Currently, at Magurele, Romania (44.35 N, 26.03 E, 90 m asl) the PBL cannot be measured directly and it is estimated from the multiwavelength Raman lidar (RALI) data, by applying the gradient method to the ratio of 1064 nm channel to 532nm channel' range corrected signal RCS_{1064}/RCS_{532p} . The results show good agreement between the data sets even though some discrepancy was found and explained.

1. INTRODUCTION

The Planetary Boundary Layer (PBL) is the part of the troposphere that is directly affected by surface conditions, ranging from several hundred meters to a few kilometers in depth, and distinguishable from the free troposphere above it by differences in flow, thermodynamic properties, and chemical content.

The structure of the PBL can be complex and variable [1;2]. Strong surface heating promotes convection that can lift the boundary layer as high as few km. At nightfall the PBL height collapses into a shallow stable boundary layer. Even where surface heating is weak, the PBL height can change significantly over time scales of hours.

Measurements, parameterizations and predictions of the height of the mixing layer (MLH) have many theoretical and practical applications such as the prediction of pollutant concentrations, the scaling of turbulence measurements and the treatment of the PBL in numerical weather prediction and climate models[3].

Continuous profile measurements for operational determination of MLH are not generally available therefore 3D numerical models are widely used in

practice for operational services. Each model uses a parameterization scheme to treat mixed layer therefore intercomparison with other methods are usually needed. Lidar data allow to test model outputs and lower the uncertainty associated to this specific parameter due to the large vertical gradient of aerosols content characterizing the interfacial region between the turbulent mixed layer and the unmixed free troposphere. In the frame of project ROMAIR LIFE08 ENV/F/000485, ARIA Technologies used mixing layer heights derived from lidar measurements over Romania for the configuration and validation of the meteorological model WRF.

In the second chapter of this paper we describe the methodology, followed by results and discussion.

The entrainment zone thickness (EZT) is the region at the top of the mixed layer where the free atmosphere above is entrained downward into the mixed layer, and thermals overshoot upward of the mixed layer. Entrainment is responsible for the growth of the PBL. Several definitions in the literature imply that the entrainment zone thickness is an average property defined over a sizable distance, area, or time [4]. Profiles from single radiosonde ascents give only rough estimates and may be completely misleading for EZT, because the radiosonde will find a very different result if it ascends in a thermal rather than between thermals [1]. Stationary ground-based remote sensors such as lidars use temporal averaging rather than horizontal spatial averaging offering better results. Measurements of the EZT are rare and are hard to validate. In the result section we attempt an intercomparison using NOAA GDAS data base and lidar measurements.

2. METHODOLOGY

2.1. Weather Research and Forecasting (WRF) model

The Weather Research and Forecasting (WRF) model is a numerical weather prediction (NWP) and atmospheric simulation system designed for both research and operational applications. There are several published comparisons of PBL height performance for the different PBL parameterization [5,6].

In this study the Planetary Boundary layer scheme used for WRF is the **Yonsei University scheme** (non-local-K scheme with explicit entrainment layer and parabolic K

profile in unstable mixed layer).

The Yonsei University PBL [7] is the next generation of the Medium Range Forecast (MRF) PBL, also using the counter gradient terms to represent fluxes due to non-local gradients. This adds to the MRF PBL[8] an explicit treatment of the entrainment layer at the PBL top. The entrainment is made proportional to the surface buoyancy flux in line with results from studies with large-eddy models [9]. The PBL top is defined using a critical bulk Richardson number of zero (compared to 0.5 in the MRF PBL), so is effectively dependent on the buoyancy profile, in which the PBL top is defined at the maximum entrainment layer (compared to the layer at which the diffusivity becomes zero). A smaller magnitude of the counter-gradient mixing in the YSU PBL produces a well-mixed boundary-layer profile, whereas there is a pronounced over-stable structure in the upper part of the mixed layer in the case of the MRF PBL.

The model output for MLH contains continuous time series.

2.2. LIDAR data

Lidar systems have been widely used to examine the structure and variability of the PBL (e.g [4], [10])

At the EARLINET Station Magurele (44.35 N, 26.03E), in the SSW part of Bucharest, we are monitoring the aerosol vertical structure using a multiwavelength Raman lidar system (RALI). RALI is a bi-axial type system [11]. The laser radiation is emitted at 1064, 532 and 355nm and collected at 1064, 532p (parralel), 532s (cross), 355, 607, 387 and 408nm. By use of combined analog and photon counting detection in combination with a total 330mJ / 9ns laser pulse and a 400mm / 4047mm focal length Cassegrain telescope, the dynamic range extends from 750m up to 15Km, depending on atmospheric conditions. The visible and infrared beams share the same transmission path, and in consequence approx. the same overlap (small differences due to different beam diameters and divergences)[12].

One of the simplest but efficient gradient methods for PBL detection involves an accurate assessment of the sharp gradients in the first derivative of the lidar range corrected signal. For the purposes of this study and to improve the regular retrieval affected by the incomplete overlap region, we applied the gradient method to the ratio of 1064 nm channel to 532nm channel's range corrected signals: RCS_{1064}/RCS_{532p} . Therefore we were able to retrieve MLH down to 200m.

For this study 100 lidar cases, spread over 3 years (2009 - 2011) have been analyzed. An interval of 30 minutes of each dataset was screened for clouds and averaged in order to obtain the final lidar range corrected signal profile.

2.3. NOAA GDAS data based

Unfortunately the models are not able to simulate the

structure of the PBL in its complexity. Therefore we used NOAA GDAS data base to compare the EZT derived from lidar measurements

National Oceanic and Atmospheric Administration's (NOAA) Global Data Assimilation System (GDAS) data were used to extract meteorological data. The National Weather Service's National Centers for Environmental Prediction (NCEP) runs a series of computer analyses and forecasts operationally. One of the operational systems is GDAS, [13] which uses the spectral Medium Range Forecast model (MRF) for the forecast. The model is run 4 times a day, global, 1 degree latitude longitude dataset on 23 pressure surfaces and basic fields such as the u- and v-wind components, temperature, and humidity.

GSI (Grid-Point Statistical Interpolation), in GDAS, is a three dimensional variational data assimilation system. GSI can assimilate (but not limited to) the following observation types: conventional observations (e.g., radiosondes, wind profilers, surface land observations, etc.), radar and satellite observations (GOES 11 and 12 sounders, AMSU-A, AMSU-B/MHS, HIRS, AIRS). Detailed information is available at <http://www.mmm.ucar.edu/mm5/mm5v3/data/gdas.html> From GDAS, the profiles of the meteorological parameters corresponding to the closest moment to the lidar measurements time were selected. This means a maximum offset of 90 min for some cases, and replication of the same meteorological profiles for other cases.

3. RESULTS AND DISCUSSIONS

3.1. MLH comparison

Mixed layer heights from long term measurements near Bucharest were compared against model simulations with WRF for 100 cases during 2009-2011 and are represented in Fig.1.

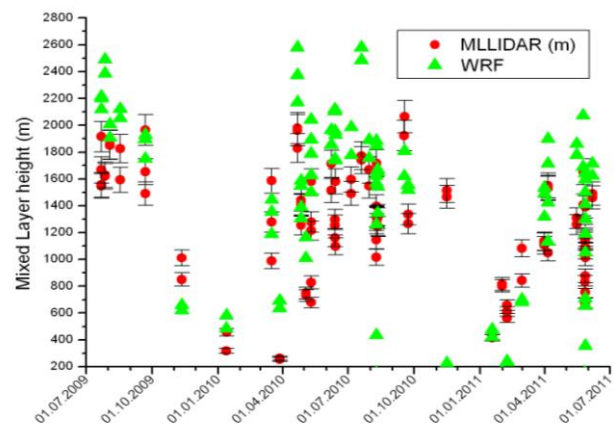


Figure 1. MLH comparison graphs with lidar – forecast 2009-2011

The correlation for all 100 cases between measured and

model MLH was quite low (R^2 about 0.5). In Fig.1 both cases when WRF (green triangles) overestimates the MLH observed and underestimates it can be noticed. Before 09:00 and after 15:00 UTC the presence or the formation of the residual layer can cause difficulties for comparison. An example of the underestimation of the MLH by the WRF model in the afternoon (15:00–18:00 UTC) is given in Fig.2. The model MLH between 15:00 and 16:00 decreases by over 1000m which is physically impossible before sunset. The high MLH from Lidar during 17:00-18:00 (after sunset) is probably related to the residual layer.

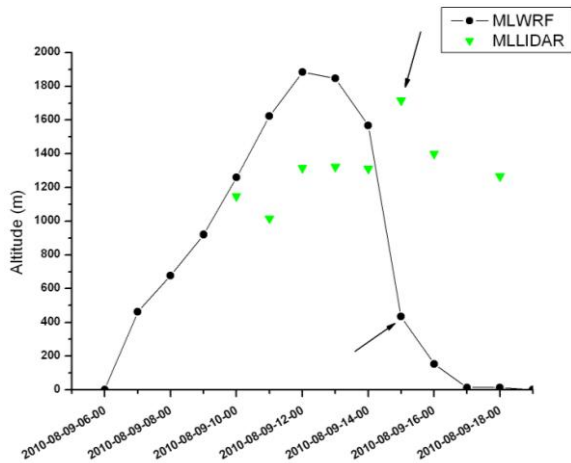


Figure 2. MLH comparison graphs with lidar and forecast of August 9th 2010

In Fig.3 there is an example when the retrieved MLH from LIDAR is much higher than the prognosis just after sunrise, indicating probably the nighttime residual layer aloft and not the stable boundary layer as is forecasted by WRF.

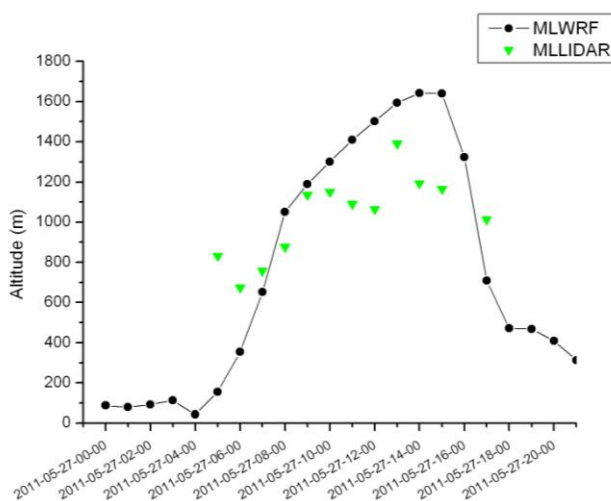


Figure 3. MLH comparison graphs with lidar and forecast of May 27th 2011

If we focus our analysis only on daytime measurements, between 9 UTC and 13 UTC (11h and 15h local time) when the MLH is usually well defined the correlation becomes much better $R^2=0.76$. There is still a large scatter in the data, the model overestimating the MLH during this phase. This is also visible in Fig.2 and 3. However the relative error is 21%, whereas the uncertainties in the model due to emission inventory are generally higher than this percentage. Disregarding the large scatter in the data, a systematic underestimation of the MLH during non-convective periods (nocturne, stable atmosphere) by the model is visible. Disagreement can be due in part to the inconsistency between the thermal or turbulence profiles and the aerosol profile.

3.2. EZT comparison

The entrainment of air from the free atmosphere into the turbulent convective boundary layer is a problem that has been considered in theoretical models, laboratory studies, field campaigns and numerical studies for many years [14].

We used NOAA GDAS data base to derive the EZT and to compare with the ones derived from lidar measurements.

Retrieval of the entrainment zone thickness using optical and meteorological parameters shows considerable scatter (correlation R^2 about 0.4). The monthly average of EZT calculated from lidar and NOAA GDAS data base between 2009 and 2011 are represented in Fig.4.

One reason of the disagreement might be that the EZT from lidar is linked to a set of boundary-layer height estimations and probably captures temporal, spatial and small-scale turbulence variations, whereas the transition-zone concept, linked to single meteorological profiles, displays only the small-scale turbulence. This was also noticed in a review by Taumner et al.[14].

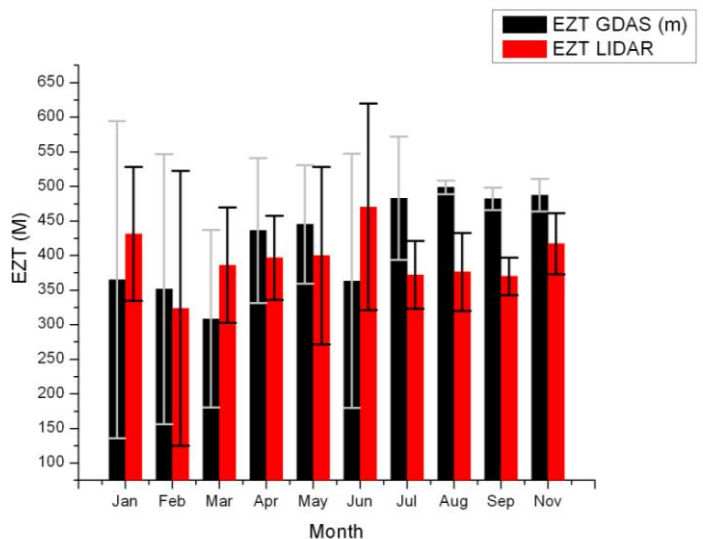


Figure 4. Monthly average of EZT comparison graphs with lidar – NOAA GDAS data base2009- 2011

4. CONCLUSIONS

Lidar systems have been widely used to examine the structure and variability of the PBL top and to derive the entrainment zone depth under well-mixed boundary layers in clear-sky conditions.

In this study a numerical weather prediction model output related to the atmospheric mixed layer height have been compared with the retrieved MLH from lidar measurements during 2009-2011. The MLH outputs from the two approaches agree well when the time span is related to the 11h and 15h local time.

During the afternoon decaying of the turbulent mixing the modeled calculates sometimes a strong drop of the MLH inconsistent with the retrieval from lidar data.

However during morning or afternoon transitions of the mixing layer, and in stable conditions, the aerosol gradients that track the layer in which turbulent mixing occurs may not be the strongest gradients of the vertical profile and therefore could be missed by the retrieval method from lidar data. MLH are systematically underestimated by the model under well-mixed boundary layers in clear-sky conditions.

Measurements of the entrainment zone thickness with lidars and the EZT derived from GDAS data base show considerable scatter, probably due to differences related to the capability of the retrieval algorithm to distinguish between various targets in the signal and/or the capability of the GDAS data to take into account local influences.

ACKNOWLEDGMENTS

The research leading to these results has received funding from the European Community's FP7-INFRASTRUCTURES-2010-1 under grant agreement number 262254 - ACTRIS and Grant no. PN 09-27 01 03.

REFERENCES

1. Stull, R. B. (1988), An Introduction to Boundary Layer Meteorology, 666pp., Dordrecht, Kluwer.
2. Sorbjan, Z. (1989), Structure of the Atmospheric Boundary Layer, 317 pp., Prentice Hall, Englewood Cliffs, N.J.
3. White J. M. and J. F. Bowers, (2009): Importance of Using Observations of Mixing Depths in order to Avoid Large Prediction Errors by a Transport and Dispersion Model, *Journal Of Atmospheric And Oceanic Technology*, **26**, pp. 22-32

4. Cohn, S. A., and W. M. Angevine, (2000): Boundary layer height and entrainment zone thickness measured by lidars and wind profiling radars. *J. Appl. Meteor.*, **39**
5. Shin H.H., S-Y. Hong, (2011) : Intercomparison of Planetary Boundary-Layer parametrizations in the WRF Model for a Single Day from CASES-99, *Boundary-Layer Meteorology* May 2011, Volume 139, Issue 2, pp 261-281
6. Shin H.H., S-Y. Hong, J. Dudhia, (2012): Impacts of the Lowest Model Level Height on the Performance of Planetary Boundary Layer Parameterizations. *Mon. Wea. Rev.*, **140**, 664–682.
7. Hong, S.-Y., Y. Noh, and J. Dudhia, (2006): A new vertical diffusion package with explicit treatment of entrainment processes. *Mon. Wea. Rev.*, **134**, 2318–2341.
8. Hong, S.-Y., and H.-L. Pan, (1996): Nonlocal boundary layer vertical diffusion in a medium-range forecast model. *Mon. Wea. Rev.*, **124**, 2322–2339.
9. Noh, Y., W. G. Cheon, S.-Y. Hong, and S. Raasch, (2003): Improvement of the K-profile model for the planetary boundary layer based on large eddy simulation data. *Bound.-Layer Meteor.*, **107**, 401–427.
10. Baars, H., Ansmann, A., Engelmann, R., and Althausen, D. (2008): Continuous monitoring of the boundary-layer top with lidar, *Atmos. Chem. Phys.*, **8**, 7281-7296, doi:10.5194/acp-8-7281-2008
11. Talianu, C., D. Nicolae, J. Ciuciu, M. Ciobanu, V. Babin, (2006): Planetary boundary layer height detection from lidar measurements, *J. Optoelectron. Adv. Mater.*, **8**, pp. 243-246
12. Radu C., L. Belegante, C. Talianu, and D. Nicolae (2010), Optimization of the multiwavelength raman lidar during EARLI09 campaign, *J. Optoelectron. Adv. Mater.* **12**(1), 165-168.
13. Kanamitsu, M., (1989): Description of the NMC global data assimilation and forecast system. *Wea. and Forecasting*, **4**, 335 - 342
14. Träumner K, Kottmeier Ch, Corsmeier U, Wieser A (2011) Convective boundary-layer entrainment: short review and progress using doppler lidar. *Boundary-Layer Meteorol.*